

# Dalton Transactions

Accepted Manuscript



This article can be cited before page numbers have been issued, to do this please use: B. Xu, W. Zhong, Z. Wei, H. Wang, J. Liu, L. Wu, Y. Feng and X. Liu, *Dalton Trans.*, 2014, DOI: 10.1039/C4DT02032D.



This is an *Accepted Manuscript*, which has been through the Royal Society of Chemistry peer review process and has been accepted for publication.

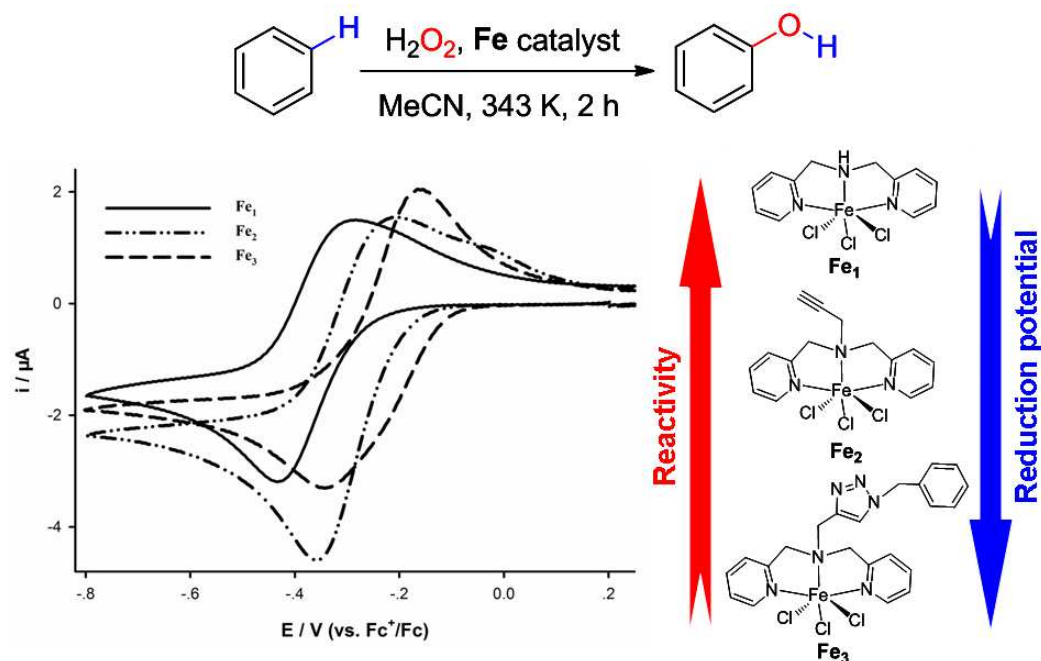
*Accepted Manuscripts* are published online shortly after acceptance, before technical editing, formatting and proof reading. Using this free service, authors can make their results available to the community, in citable form, before we publish the edited article. We will replace this *Accepted Manuscript* with the edited and formatted *Advance Article* as soon as it is available.

You can find more information about *Accepted Manuscripts* in the [Information for Authors](#).

Please note that technical editing may introduce minor changes to the text and/or graphics, which may alter content. The journal's standard [Terms & Conditions](#) and the [Ethical guidelines](#) still apply. In no event shall the Royal Society of Chemistry be held responsible for any errors or omissions in this *Accepted Manuscript* or any consequences arising from the use of any information it contains.

## Graphical Abstract

## Iron (III) complexes of multidentate pyridinyl ligand: Synthesis, characterization and catalysis on the direct hydroxylation of benzene

Beibei Xu<sup>a</sup>, Wei Zhong<sup>b,c</sup>, Zhenhong Wei<sup>a</sup>, Hailong Wang<sup>b</sup>, Jian Liu<sup>a</sup>, Li Wu<sup>a</sup>, Yonggang Feng<sup>b</sup> andXiaoming Liu<sup>a,b,\*</sup>

The correlation between the electrochemistry of multidentate pyridinyl iron complexes  $\text{Fe}_1$ - $\text{Fe}_3$  and their catalytic performance on the direct hydroxylation of benzene into phenol suggests that increasing the electron-donating capability of the ligands coordinating to the metal centre is beneficial to improving the catalysis.

Cite this: DOI: 10.1039/C4DT02032D

www.rsc.org/xxxxxx

ARTICLE TYPE

# Iron (III) complexes of multidentate pyridinyl ligand: Synthesis, characterization and catalysis on the direct hydroxylation of benzene

Beibei Xu,<sup>a</sup> Wei Zhong,<sup>b,c</sup> Zhenhong Wei,<sup>a</sup> Hailong Wang,<sup>b</sup> Jian Liu,<sup>a</sup> Li Wu,<sup>a</sup> Yonggang Feng<sup>b</sup> and Xiaoming Liu<sup>a,b,\*</sup>

Received (in XXX, XXX) Xth XXXXXXXXX 20XX, Accepted Xth XXXXXXXXX 20XX

DOI: 10.1039/b000000x

Three multidentate ligands **L**<sub>1</sub>–**L**<sub>3</sub> derived from bis(pyridin-2-ylmethyl)amine (**L**<sub>1</sub>) were synthesized. Reaction of these ligands with FeCl<sub>3</sub>·6H<sub>2</sub>O in methanol led to the formation of iron complexes **Fe**<sub>1</sub>–**Fe**<sub>3</sub> (**Fe**<sub>1</sub>: [Fe**L**<sub>1</sub>Cl<sub>3</sub>]; **Fe**<sub>2</sub>: [Fe**L**<sub>2</sub>Cl<sub>3</sub>]; **Fe**<sub>3</sub>: [Fe**L**<sub>3</sub>Cl<sub>3</sub>]) in good yields, respectively. These complexes have been fully characterized. The structures of complexes **Fe**<sub>1</sub>–**Fe**<sub>3</sub> have been determined using X-ray single crystal diffraction analysis. Electrochemical investigation revealed that complex **Fe**<sub>3</sub> forms partially **Fe**<sub>4</sub> ([Fe**L**<sub>3</sub>Cl<sub>2</sub>](PF<sub>6</sub>)) by the replacement of one of its three chlorides with its pendant triazolyl group in solution. **Fe**<sub>4</sub> was also synthesized by dechlorination using AgPF<sub>6</sub> as the Cl<sup>–</sup> abstractor and its composition was further confirmed by both elemental analysis and X-ray single crystal diffraction analysis. All the four complexes catalyze direct hydroxylation of benzene to phenol with hydrogen peroxide as an oxidant in a mixed medium of water and acetonitrile. The reactivity of the complexes correlates well to their reduction potentials. The more negative the potential, the more reactive (high conversion rate) the catalysts. These complexes catalyze not only the oxidation of benzene, but also the further oxidation of the product phenol. In the oxidation, radical mechanism is certainly involved but alternative pathway may also exist.

## 1. Introduction

Iron is one of the most abundant metals on earth and has a number of advantages over other transition metals as a catalyst, for example, readily availability, low cost and environmentally benign probably due to its good abundance. In nature, iron is an indispensable element in many living organisms as the metal centers of many enzymes. These enzymes play important biological roles by catalyzing many essential reactions in living organisms. For example, cytochrome P450 oxidizes selectively the long aliphatic side chain of cholesterol in the biosynthesis of female hormone progesterone.<sup>1</sup> Methane monooxygenase, an enzyme containing a diiron core, converts methane into methanol as part of the metabolism of methanotrophs.<sup>2</sup> Hydrogenases are also iron-containing enzymes and catalyze both evolution and oxidation of hydrogen at remarkable efficiency and rate.<sup>3</sup> In principle, iron-based systems ought to have great potentials as efficient, affordable and safe catalysts in industry.

Phenol is widely used in industry as an important chemicals for the production of phenol resins, fibers, dyestuffs and medicines.<sup>4</sup> Currently, phenol is mainly manufactured by a three-step cumene process.<sup>5,6</sup> Its major problems are low yield (~5% based on the amount of benzene initially used), high energy consumption and production of an equal amount of acetone as its by-product. Therefore, it is extremely desirable to find alternative ways for its production, which can ideally overcome the disadvantages of the

cumene process. It is understandable that direct hydroxylation of benzene, in the viewpoint of atomic economy, is the most efficient way for the production of phenol. In this process, one of the C–H bonds is activated and then hydroxylated. However, the high bond energy (460 kJ mol<sup>–1</sup>) makes it impossible without the help of a catalyst. Both heterogeneous and homogeneous catalysts have been investigated to achieve this direct hydroxylation. The heterogeneous catalysts such as TS-1,<sup>7–9</sup> SBA-15<sup>10,11</sup> and other molecular sieves,<sup>12–14</sup> hydrotalcites,<sup>15</sup> and MWCNTs<sup>16,17</sup> loaded with metal ions have shown high efficiency. But leaching of active species hinders their further application at an industrial scale. Furthermore, their catalytic performances could highly depend on their preparations. Homogeneous catalysts, however, possess a number of advantages, for example, operational under mild conditions, tunable in catalytic performance through ligand design.<sup>18–21</sup> By appropriately selecting a metal ion, catalytic performance could be further improved.<sup>20,21</sup> But to date, only limited reports have been devoted to developing homogeneous catalysts.<sup>18–24</sup> The advantages of the homogeneous systems need to be further exploited.

As aforementioned, iron-based catalytic systems have great potentials as catalysts. Additionally, iron is one of the essential metals in our own bodies. Therefore, it ought to possess the least detrimental effect towards our environment as well as living organisms. Indeed, among the reported homogeneous catalysts, iron complexes showed promising efficiency in catalyzing the

direct hydroxylation of benzene.<sup>23, 24</sup> In nature, it is not uncommon that iron is employed as a catalytic centre to activate C–H bond. For example, cytochromes P-450, non-heme iron mono- and dioxygenases perform hydroxylation of aromatic compounds *via* C–H bond activation.<sup>25, 26</sup> Both the natural systems and synthetic catalysts suggest that iron complexes could be effective catalysts for the conversion of benzene to phenol if the ligands are appropriately designed and both the electronic and steric properties of the complexes are satisfactorily tuned. Under these inspirations, we are prompted to develop iron-based homogeneous catalysts for benzene hydroxylation and explore the correlations between the catalytic efficiency and both electronic and structural features of the iron-based catalysts. Herein, we report three multidentate pyridinyl ligands **L**<sub>1</sub>–**L**<sub>3</sub> and their Fe(III) complexes **Fe**<sub>1</sub>–**Fe**<sub>4</sub>. Complex **Fe**<sub>4</sub> was derived from **Fe**<sub>3</sub> by the substitution of one of the bound chlorides by the pendant triazolyl group. The catalysis of these complexes towards the oxidation of benzene by H<sub>2</sub>O<sub>2</sub> to phenol was investigated. Their catalysis and relevance to both electrochemistry and structures were also discussed. Among the four complexes, complex **Fe**<sub>2</sub> exhibited the best yield in terms of the production of phenol whereas **Fe**<sub>1</sub> is the most active one which is of the most negative reduction potential.

## 2. Experimental

### 2.1 General procedures and computations

All chemicals and solvents were of AR grade and purchased from local suppliers unless otherwise stated. The organic solvents used in this work were appropriately dried when necessary. Ligands **L**<sub>1</sub>–**L**<sub>3</sub><sup>27–29</sup> and their Fe(III) complexes **Fe**<sub>1</sub>–**Fe**<sub>3</sub><sup>30</sup> were synthesized following literature procedures with modifications. Elemental analyses were performed on a CHN elemental analyzer (Elementar Vario MICRO). FTIR spectra were recorded on Agilent 640 using a CaF<sub>2</sub>-cell with a spacer of 0.1 mm. UV-vis spectra were recorded in the range of 200–800 nm on a spectrophotometer (VARIAN 50 Conc) in acetonitrile. Crystallographic data of complexes **Fe**<sub>1</sub>–**Fe**<sub>4</sub> were collected on a Bruker SMART CCD diffractometer with graphite-monochromated Mo–K $\alpha$  radiation ( $\lambda$  = 0.71073 Å). The crystal structures were solved using direct methods in SHELXS and refined by full-matrix least-squares routines, based on  $F^2$ , using the SHELXL package.<sup>31</sup> The crystallographic data of complexes **Fe**<sub>1</sub>–**Fe**<sub>4</sub> were deposited in the Cambridge Crystallographic Data Center (CCDC 997390–997393).

Electrochemistry was performed in a gas-tight three-electrode system in which a vitreous carbon disk ( $\phi$  = 1 mm) was used as a working electrode, a carbon strip as counter electrode, and Ag / AgCl (inner reference solution : 0.45 mol L<sup>–1</sup> [NBut<sub>4</sub>]BF<sub>4</sub> + 0.05 mol L<sup>–1</sup> [NBut<sub>4</sub>]Cl in dichloromethane) against which the potential of ferrocenium / ferrocene couple is 0.55 V in 0.1 mol L<sup>–1</sup> [NBut<sub>4</sub>]BF<sub>4</sub> in acetonitrile as described elsewhere.<sup>32, 33</sup> Ferrocene was added as an internal standard, and all potentials are quoted against ferrocenium / ferrocene couple (Fc<sup>+</sup> / Fc).

In theoretic calculations, **Fe**<sub>3</sub> and **Fe**<sub>4</sub> in neutral and reduced states were fully optimized in gas phase without any symmetry constraints at the (U)BP86 / TZVP level of theory.<sup>34, 35</sup> The

atomic coordinates in neutral state are derived from corresponding crystal structures. The initial geometries of the reduced states were approximately established using the crystal structure parameters of their parent complexes. Vibrational frequencies were calculated based on the optimized geometries and the absence of negative frequencies confirmed that the structures were local minimum–energy structures.

The free energies of solvation ( $\Delta G$ ) of **Fe**<sub>3</sub> and **Fe**<sub>4</sub> in different states were evaluated by the self-consistent reaction field (SCRF) approach based on the integral equation formalism of the polarized continuum model (IEFPCM) level of theory using the keyword SCFVAC. The choice of solvent was acetonitrile in which the electrochemistry of the complexes was performed. To calculate the one–electron reduction potential, the free energy changes in the reduction processes were calculated by using Born–Haber cycle.<sup>36</sup> The calculated potentials ( $E_{1/2}$ ) are calibrated against Fc<sup>+</sup> / Fc whose absolute oxidation potential is –4.81 V calculated using the same approach as that for **Fe**<sub>3</sub> and **Fe**<sub>4</sub>. All calculations were carried out using Gaussian 03 program.<sup>37</sup>

### 2.2 Synthesis

**2.2.1 Preparation of bis(pyridin-2-ylmethyl)amine (**L**<sub>1</sub>).** 2-Picolinaldehyde (2.5 mL, 26 mmol) was added to a solution of 2-pyridylmethylamine (2.7 mL, 26 mmol) in MeOH (15 mL), which was stirred for 6 h at room temperature before sodium borohydride (2.4 g, 63.8 mmol) was added to the mixture at ice-temperature. The reaction mixture was further stirred at room temperature overnight. After removal of the solvents under reduced pressure, 30 mL of distilled water was added, and then extracted successively with dichloromethane (30 mL  $\times$  3). All the extracts were combined before being dried with MgSO<sub>4</sub>. Removal of the solvents under reduced pressure gave a crude product which was further purified using flash chromatography on silica gel column (eluent: ethyl acetate / ethanol / triethylamine = 5 : 1 : 0.1) to produce yellow oily liquid (3.32 g, 54%). <sup>1</sup>H NMR (400 MHz, CDCl<sub>3</sub>)  $\delta$  8.47 (d,  $J$  = 4.7 Hz, 2H, py), 7.55 (t,  $J$  = 7.6 Hz, 2H, py), 7.28 (s, 2H, py), 7.14–6.98 (m, 2H, py), 3.90 (s, 4H, CH<sub>2</sub>), 2.86 (s, 1H, NH).

**2.2.2 Preparation of N,N-bis(pyridin-2-ylmethyl)prop-2-yn-1-amine (**L**<sub>2</sub>).** 3-Bromopropyne (0.42 mL, 5.3 mmol) was added to the mixture of **L**<sub>1</sub> (1.05 g, 5.3 mmol) and K<sub>2</sub>CO<sub>3</sub> (0.73 g, 5.3 mmol) in THF (20 mL) in a round bottom flask (100 mL). The reaction was refluxed for 24 h before removal of the solvents under reduced pressure to give a crude product. The product was further purified using flash chromatography on silica gel column (eluent: ethyl acetate / ethanol / triethylamine = 15 : 1 : 0.1) to produce a yellow oily liquid (0.73 g, 58%). IR (DCM,  $\nu$ /cm<sup>–1</sup>): 3297, 2839, 2106 and 1591. <sup>1</sup>H NMR (400 MHz, CDCl<sub>3</sub>)  $\delta$  8.58 (d,  $J$  = 4.7 Hz, 2H, py), 7.68 (td,  $J$  = 7.6, 1.6 Hz, 2H, py), 7.54 (d,  $J$  = 7.8 Hz, 2H, py), 7.21 – 7.16 (m, 2H, py), 3.94 (s, 4H, CH<sub>2</sub>), 3.45 (d,  $J$  = 2.3 Hz, 2H, CH<sub>2</sub>), 2.32 (t,  $J$  = 2.3 Hz, 1H, CH).

**2.2.3 Preparation of Azidomethylbenzene (**1**).** A solution of bromomethylbenzene (1.71 g, 10 mmol) and sodium azide (1.30 g, 20 mmol) in DMF (5 mL) was stirred at room temperature for 24 h. The reaction was diluted with water (5 mL) and extracted with diethylether (4  $\times$  10 mL). The organic fractions were combined and washed successively with water (4  $\times$  10 mL), dried with anhydrous magnesium sulfate (MgSO<sub>4</sub>) and concentrated *in*



*vacuo* to produce azidomethylbenzene (**1**) as a yellow liquid (1.14 g, 85%). The compound was used in next reaction without further purification. IR (DCM,  $\nu/\text{cm}^{-1}$ ): 3032, 2096, 1496 and 1455.

**2.2.4 Preparation of 1-(1-benzyl-1H-1,2,3-triazol-4-yl)-N,N-bis(pyridin-2-ylmethyl)methanamine (**L<sub>3</sub>**).** A solution of compound **1** (283 mg, 2.2 mmol) in THF (2 mL) was added to the solution of ligand **L<sub>2</sub>** (474 mg, 2 mmol) in THF (3 mL), followed by the addition of a mixture of CuI (38 mg, 0.2 mmol) and Et<sub>3</sub>N (2.5 mL, 2.2 mmol) in THF (2 mL). After being stirred for 18 h at 40 °C, the yellow reaction solution turned to a black suspension. Removal of the solvents under reduced pressure gave a crude product which was further purified using flash chromatography on silica gel column (eluent: ethyl acetate / ethanol / triethylamine = 15 : 1 : 0.1) to produce a yellow oily liquid (303 mg, 41%). <sup>1</sup>H NMR (400 MHz, CDCl<sub>3</sub>)  $\delta$  8.44 (d,  $J$  = 4.4 Hz, 2H, py), 7.55 (tt,  $J$  = 14.1, 7.1 Hz, 2H, py), 7.51 – 7.39 (m, 3H, ph), 7.33 – 7.21 (m, 2H, py, 1H, CH), 7.22 – 7.13 (m, 2H, py), 7.06 (dd,  $J$  = 6.7, 5.5 Hz, 2H, ph), 5.45 (s, 2H, CH<sub>2</sub>), 3.79 (d,  $J$  = 8.2 Hz, 2H, CH<sub>2</sub>), 3.76 (s, 4H, CH<sub>2</sub>). <sup>13</sup>C NMR (101 MHz, CDCl<sub>3</sub>)  $\delta$  159.09, 148.96, 144.66, 136.42, 134.78, 128.99, 128.56, 127.87, 123.22, 122.95, 121.98, 77.44, 77.12, 76.80, 59.54, 53.96, 48.59.

**2.2.5 Preparation of complexes [FeL<sub>1</sub>Cl<sub>3</sub>](Fe<sub>1</sub>), [FeL<sub>2</sub>Cl<sub>3</sub>](Fe<sub>2</sub>) and [FeL<sub>3</sub>Cl<sub>3</sub>](Fe<sub>3</sub>).** A solution of FeCl<sub>3</sub>·6H<sub>2</sub>O (542 mg, 2 mmol) in methanol (2 mL) was mixed with a methanolic solution (3 mL) of an equivalent of **L<sub>1</sub>** (398 mg, 2 mmol). The reaction was stirred for 3 h to produce a dark-yellow precipitate **Fe<sub>1</sub>** (625 mg, 87%), which was collected by filtration, washed successively with methanol, dichloromethane and tetrahydrofuran, and dried *in vacuo*. Crystals suitable for X-ray single crystal diffraction analysis were obtained from its solution in a mixture DMF / diethyl ether at room temperature. Elemental analysis for **Fe<sub>1</sub>** (C<sub>12</sub>H<sub>13</sub>Cl<sub>3</sub>FeN<sub>3</sub>, FW = 361.46): calc., C%, 39.87, H%, 3.63, N%, 11.63; found, C%, 40.06, H%, 3.60, N%, 11.22.

**Fe<sub>2</sub>** (637 mg, 80%) and **Fe<sub>3</sub>** (763 mg, 72%) were analogously synthesized using the same procedure as described for the preparation of **Fe<sub>1</sub>**. Crystals of complex **Fe<sub>2</sub>** suitable for X-ray analysis single crystal diffraction were obtained from its solution in a mixture of acetonitrile / diethyl ether in few days at room temperature. Elemental analysis for **Fe<sub>2</sub>** (C<sub>15</sub>H<sub>15</sub>Cl<sub>3</sub>FeN<sub>3</sub>, FW = 399.50): calc., C%, 45.10, H%, 3.78, N%, 10.52; found, C%, 45.01, H%, 3.81, N%, 10.30. Crystals of complex **Fe<sub>3</sub>** suitable for X-ray single crystal diffraction analysis were obtained from its solution in a mixture of dichloromethane/diethyl ether in few days at room temperature. Elemental analysis for **Fe<sub>3</sub>** (C<sub>22</sub>H<sub>22</sub>Cl<sub>3</sub>FeN<sub>6</sub>, FW = 532.65): calc., C%, 49.61, H%, 4.16, N%, 15.78; found, C%, 50.09, H%, 4.37, N%, 15.79.

**2.2.6 Preparation of complex [FeL<sub>3</sub>Cl<sub>2</sub>]PF<sub>6</sub> (**Fe<sub>4</sub>**).** A solution of AgPF<sub>6</sub> (72 mg, 0.28 mmol) in acetonitrile (4 mL) was added to a solution of complex **Fe<sub>3</sub>** (151 mg, 0.28 mmol) in acetonitrile (2 mL). The solution was stirred for 6 h. An inorganic solid (AgCl) was filtered off and the filtrate was concentrated *in vacuo* to give a yellow solid (133 mg, 74%), which was washed, in portions, with a small amount of cold petroleum ether and diethyl ether, respectively. Crystals suitable for X-ray single crystal diffraction analysis were obtained from its solution in a mixture of dichloromethane/methanol in few days at room temperature. Elemental analysis for **Fe<sub>4</sub>** (C<sub>22</sub>H<sub>22</sub>Cl<sub>2</sub>F<sub>6</sub>FeN<sub>6</sub>P, FW = 642.18): calc., C%, 41.15, H%, 3.45, N%, 13.09; found, C%, 41.09, H%,

3.58, N%, 12.63.

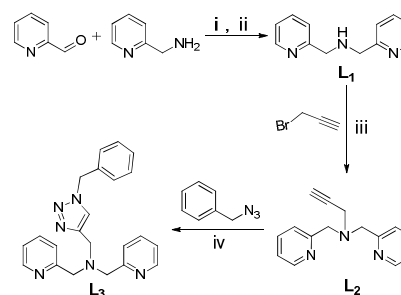
## 2.3 Catalytic assessment

A typical procedure is as follows: benzene (0.9 mL, 10 mmol), acetonitrile (3.8 mL) and catalytic amount of the iron (III) complex (0.2 mol%) were placed into a reaction vessel (10 mL) equipped with cooling condenser and placed in an oil-bath. The reaction was heated at appropriate temperature for period of a time. When the reaction reached the specified temperature, aqueous H<sub>2</sub>O<sub>2</sub> (30 wt%, 1.2 mL, 12 mmol) was slowly and carefully added in one-go. When the reaction was stopped, the volume was calibrated to 10 mL with CH<sub>3</sub>CN. To the calibrated reaction solution was added MgSO<sub>4</sub> (3 g) to remove the water in the reaction before being analyzed by gas chromatography (GC 6890) with a packed column of Restek capillary SE-54 and using toluene as an internal standard. The temperature of the GC column was set at 60 °C for 1 min and then was programmed to rise to 160 °C at the rate of 10 °C min<sup>-1</sup>. Under the employed conditions, the retention time for benzene, toluene, benzoquinone and phenol were 3.3 ± 0.2 min, 4.4 ± 0.2 min, 6.6 ± 0.2 min, and 7.4 ± 0.2 min, respectively.

In establishing the calibration curves for quantitative analysis of both benzene and phenol, 5 standard samples containing quantitative benzene, phenol and toluene, respectively, were prepared in appropriate ratios, heated and worked up in the same manner as that for the above reaction. The samples were analyzed by GC with the same GC parameters. Plotting the ratios of area-readings of benzene and phenol over that of toluene, respectively, against their quantities in the standard samples produced two linear equations,  $y_b = 0.0054 x_b - 0.0183$  ( $R = 0.9986$ ) and  $y_p = 0.0022 x_p - 0.0631$  ( $R = 0.9982$ ) for benzene and phenol, respectively, where  $y$  is designated as the area-reading,  $x$  as the quantity of the substances, and  $b$  stands for benzene and  $p$  for phenol. The two calibrating equations were used to quantitative analysis of the two substances in all samples. To calibrate any uncertainty resulting from batches, a synthesized sample was always analyzed along with reaction samples in each batch. Reaction yield / selectivity and conversion rate are calculated as follows: phenol (mmol) / benzene-reacted (mmol) × 100% and benzene-reacted (mmol) / benzene initially used (mmol) × 100%, respectively.

## 3. Results and discussion

### 3.1 Synthesis and characterization

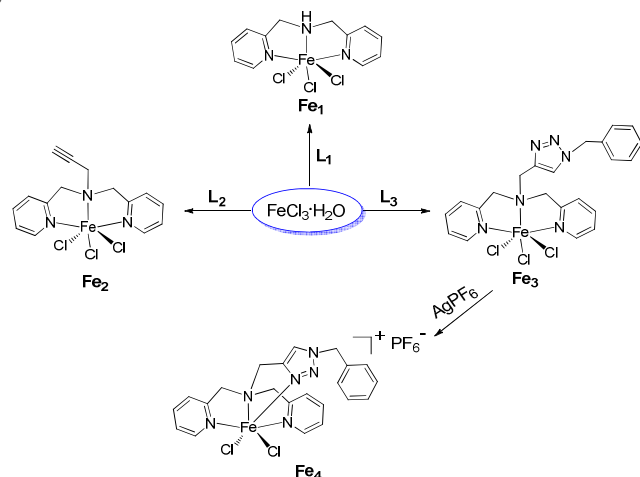


**Scheme 1** Synthesis of ligands **L<sub>1</sub>**–**L<sub>3</sub>**. Reaction conditions: i, MeOH, room temperature; ii, NaBH<sub>4</sub>; iii, K<sub>2</sub>CO<sub>3</sub>, THF, room temperature; iv, CuI, Et<sub>3</sub>N, THF, 40 °C.

The three ligands **L**<sub>1</sub>-**L**<sub>3</sub> were prepared following the literature procedures,<sup>27-29</sup> Scheme 1. **L**<sub>1</sub> was prepared by first forming a Schiff base and then reduction by NaBH<sub>4</sub>. Since the reduction involving hydrogen gas evolution, the addition of NaBH<sub>4</sub> was carried out in portions with care and the reaction was kept at ice-temperature. Reaction of the secondary amine (**L**<sub>1</sub>) with 3-bromopropyne led to ligand **L**<sub>2</sub>. Ligand **L**<sub>3</sub> was prepared by reacting ligand **L**<sub>2</sub> with azidomethylbenzene via “click reaction”.

Complexes **Fe**<sub>1</sub>-**Fe**<sub>3</sub> were synthesized from the reaction of ligands (**L**<sub>1</sub>-**L**<sub>3</sub>) with FeCl<sub>3</sub>·6H<sub>2</sub>O, respectively, in methanol. All the three complexes adopt octahedral coordination geometry as revealed by their crystal structures (Fig. 1). The structural similarity is also reflected in their UV-vis spectrum (Fig. S1).

When the secondary amine of ligand **L**<sub>1</sub> is converted into tertiary amine (**L**<sub>2</sub> and **L**<sub>3</sub>), the solubility of their corresponding iron (III) complexes differs drastically. **Fe**<sub>1</sub> is soluble in DMF but hardly soluble in other common solvents. But **Fe**<sub>2</sub> and **Fe**<sub>3</sub> have much improved solubility, which are soluble in most organic solvents, for example, acetonitrile, ethanol and dichloromethane. The improvement ought to be attributed to the further introducing of organic moieties into the ligands. Complex **Fe**<sub>4</sub> was prepared from complex **Fe**<sub>3</sub> in good yield by using one equivalent of AgPF<sub>6</sub>, Scheme 2.



Scheme 2 Synthesis of iron complexes **Fe**<sub>1</sub>-**Fe**<sub>4</sub>.

### 3.2 Structural analysis

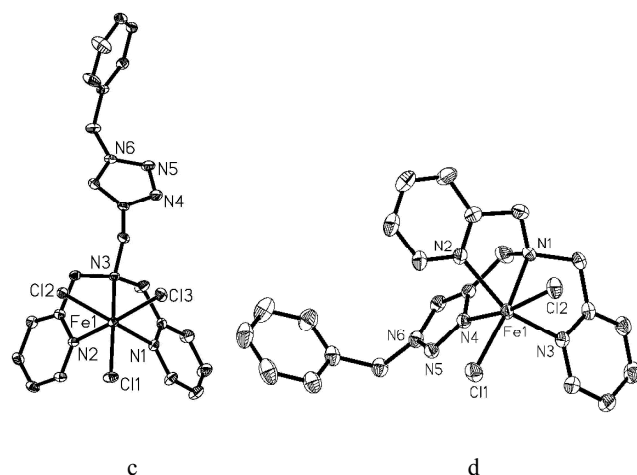
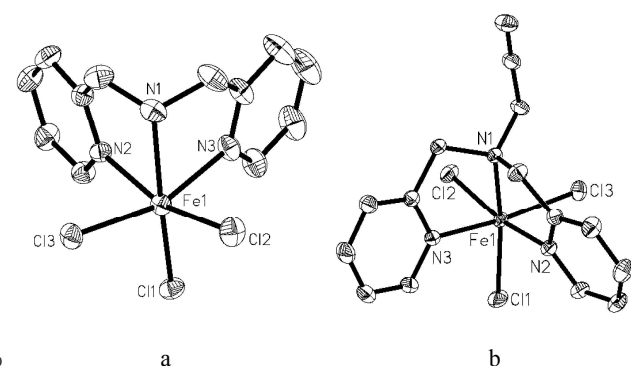


Fig. 1 Crystal structures of complexes **Fe**<sub>1</sub> (a), **Fe**<sub>2</sub> (b), **Fe**<sub>3</sub> (c) and **Fe**<sub>4</sub> (d).

Details of the crystallographic data of complexes **Fe**<sub>1</sub>-**Fe**<sub>4</sub> are summarized in Table 1. Selective bonding parameters for complexes **Fe**<sub>1</sub>-**Fe**<sub>4</sub> are tabulated in Table 2. The structural views of complexes **Fe**<sub>1</sub>-**Fe**<sub>4</sub> are shown in Fig. 1. As shown in Fig. 1, the complexes **Fe**<sub>1</sub>-**Fe**<sub>3</sub> are mononuclear and adopt an octahedral geometry with the same donor-set, “N<sub>3</sub>-Cl<sub>3</sub>”, and the complex **Fe**<sub>4</sub> with “N<sub>4</sub>-Cl<sub>2</sub>”. Due to the π-accepting nature of the pyridinyl ring, the distances of Fe(1)-N(2) and Fe(1)-N(3) bonds assigned to Fe-N(Py) in complexes **Fe**<sub>1</sub>-**Fe**<sub>4</sub> are slightly shorter than the Fe(1)-N(1).

### 3.3 Electrochemistry

In the direct hydroxylation of benzene catalyzed by a transition metal complex, the step of binding of the oxidant H<sub>2</sub>O<sub>2</sub> to the metal center is essential.<sup>38</sup> Therefore, the electron density on the metal center ought to have influence on its catalysis. And the electron density is certainly correlated to the capability of its accepting electron. Thus, it is worthy of examining the electrochemistry of these complexes. In acetonitrile, all the complexes exhibited a quasi-reversible reduction process between -0.5 and -0.3 V, Fig. 2. But further looking into the electrochemistry of complex **Fe**<sub>3</sub> reveals that its reduction is composed of at least two processes. To find out what happened, its electrochemistry was examined at various scanning rates and temperatures, Figs. 3 and 4. The results shown in Figs. 3 and 4 indicate that both increasing the scanning rate and lowering the temperature could suppress the first reduction, which suggests a chemical reaction is involved. As revealed by its crystal structure (Fig. 1), **Fe**<sub>3</sub> possesses a free triazolyl group which is both a σ-donor and π-acceptor. If one of the three chlorides bound in **Fe**<sub>3</sub> could dissociate, the pendant triazolyl group would readily move in to replace the dissociated chloride. Since chloride is a π-donor, its substitution by the triazolyl group will certainly shift positively the reduction potential of the product. The irreversibility of the second reduction and the relation of the reduction and the oxidation potentials allow us proposing the mechanism of electron transfer and the coupled chemical reaction, Scheme 3. To confirm the proposed mechanism, one chloride was abstracted from **Fe**<sub>3</sub> using one molar equivalent of AgPF<sub>6</sub> to give a yellow solid. Micro analysis results indicate that

its composition is in agreement with that defined by  $[\text{FeL}_3\text{Cl}_2]\text{PF}_6$  ( $\text{Fe}_4$ ) whose absolute structure was also determined crystallographically (Fig. 1). By adding the complex into the solution of  $\text{Fe}_3$ , it was found out that the first reduction was enhanced as suggested by the pulse differential voltammograms, Fig. 5. To further rationalize the mechanism depicted in Scheme 3, DFT calculations were performed. The results show, indeed, that dissociating a chloride from  $\text{Fe}_3$  followed by the binding of the pendant triazolyl group to form  $\text{Fe}_4$  is thermodynamically favored. But the tendency of “kicking” out a chloride from its reduced form  $\text{Fe}_3^-$  is much stronger as suggested by the large Gibbs free energy of the process. This is sensible since upon reduction, the electron density on the metal centre increases further and cleaving a chloride will off-set this increase in electron density. The theoretical results alongside with the experimental observations validate firmly the mechanism shown in Scheme 3.

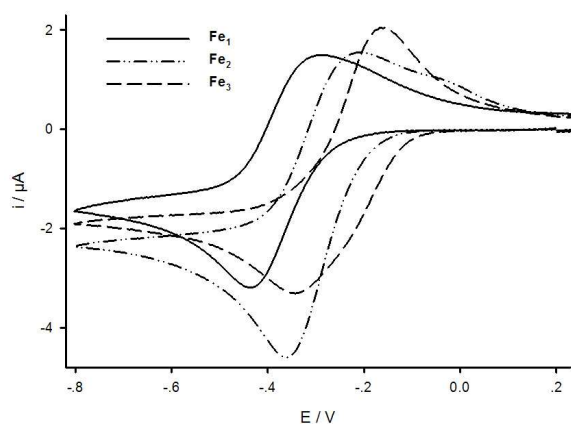


**Fig. 2** Cyclic voltammograms of complexes  $\text{Fe}_1$  ( $2.94 \text{ mmol L}^{-1}$ ),  $\text{Fe}_2$  ( $2.93 \text{ mmol L}^{-1}$ ) and  $\text{Fe}_3$  ( $2.91 \text{ mmol L}^{-1}$ ) in acetonitrile ( $\nu = 0.1 \text{ V s}^{-1}$ , 298 K).

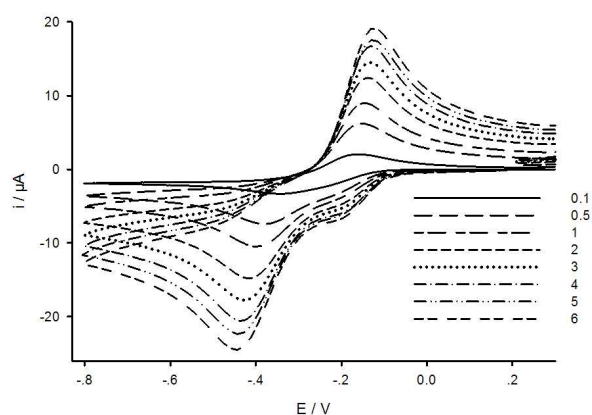


**Fig. 3** Cyclic voltammograms of complex  $\text{Fe}_3$  ( $2.91 \text{ mmol L}^{-1}$ ) in acetonitrile at various scanning rates: 0.1, 0.5, 1.0, 2.0, 3.0, 4.0, 5.0 and  $6.0 \text{ V s}^{-1}$ .

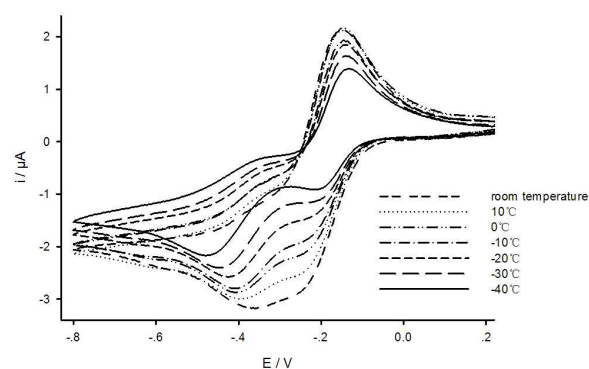


**Fig. 4** Cyclic voltammograms of complex  $\text{Fe}_3$  ( $2.91 \text{ mmol L}^{-1}$ ) in acetonitrile at various temperatures: room temperature, 10, 0, -10, -20, -30 and  $-40 \text{ }^\circ\text{C}$ .

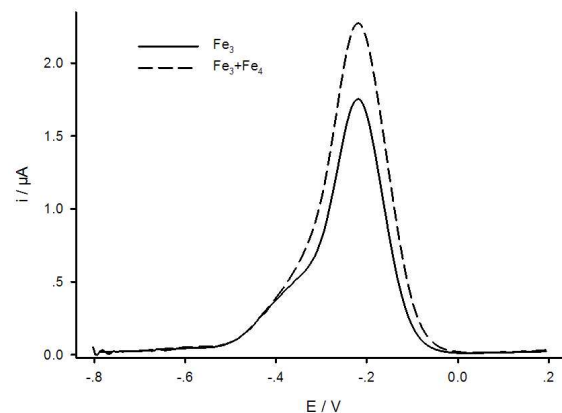
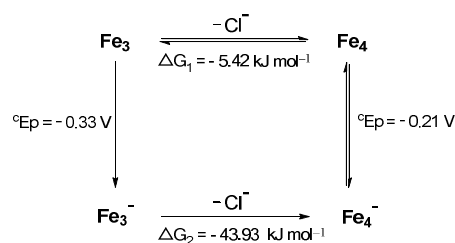


**Fig. 5** Differential pulse voltammograms of complex  $\text{Fe}_3$  ( $2.86 \text{ mmol L}^{-1}$ ) and  $\text{Fe}_3$  ( $2.86 \text{ mmol L}^{-1}$ ) +  $\text{Fe}_4$  ( $1.29 \text{ mmol L}^{-1}$ ) in acetonitrile ( $\nu = 0.1 \text{ V s}^{-1}$ , 298 K).



**Scheme 3** Mechanism of electron transfer and the coupled chemical reaction. Please note that both reduction peak potentials were quoted for consistence.

### 3.4 Catalytic hydroxylation of benzene to phenol

The catalytic activity of the complexes was assessed using benzene oxidation reaction by  $\text{H}_2\text{O}_2$  in acetonitrile. Reaction conditions for the catalysis were optimized using  $\text{Fe}_2$  as a catalyst. Full details of the optimization are given in supporting information. Throughout the work, reaction temperature and time are set at  $70 \text{ }^\circ\text{C}$  and 2h, respectively, and the quantities of other components are as follows, the catalyst (equivalent of iron: 0.02 mmol), benzene (0.9 mL, 10 mmol),  $\text{H}_2\text{O}_2$  (1.2 mL, 12 mmol)

and solvent acetonitrile (3.8 mL).

Selecting an appropriate quantity of the oxidant is a dilemma as decreasing the oxidant would improve the selectivity but the conversion rate would drop as shown in Table 3. The root cause of this is that the product phenol undergoes further catalytic oxidation. Varying the amount of the catalyst does not significantly alter the conversion rate of benzene, Fig. 6. But for the reaction yield / selectivity, 0.2%-0.3% of the examined catalyst gave relatively good results. Thus, throughout the investigation, 0.2% was used for all the complexes.

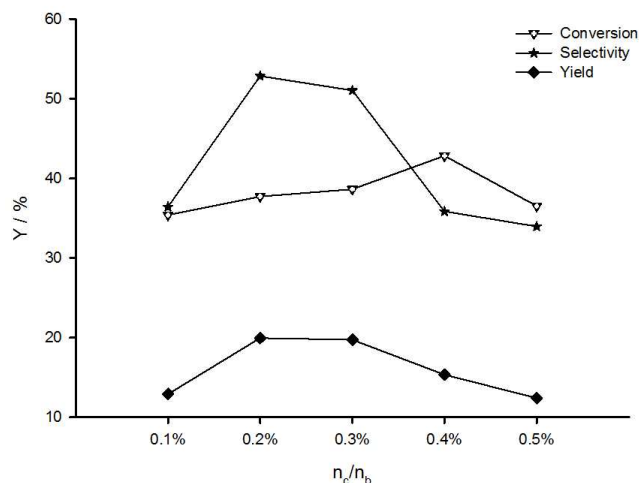


**Fig. 6** Variations of the conversion rate and yield / selectivity with the quantity of the catalyst ( $\text{Fe}_2$ ) used. ( $n_c$ : mole of  $\text{Fe}_2$ ,  $n_b$ : mole of benzene). Reaction conditions:  $\text{H}_2\text{O}_2$  (1.2 mL, 12 mmol), benzene (0.9 mL, 10 mmol), and acetonitrile (3.8 mL), 70 °C, 2h.

Under the optimized conditions, the catalytic activities of the three complexes were examined. For comparison, complex  $\text{Fe}_4$  generated from  $\text{Fe}_3$  by abstracting one of the three chlorides was also investigated. All the results are tabulated in Table 3. It is found that  $\text{Fe}_2$  shows the best catalytic performance. Although all the systems do not show excellent performance in both selectivity and reaction yield, complex  $\text{Fe}_2$  exhibits the best reaction yield and selectivity. It must be pointed out that no significant variation in performance was observed for all the complexes. This is probably due to that all the complexes ( $\text{Fe}_1$ - $\text{Fe}_3$ ) are highly similar in both structure and coordinating atmosphere. As shown in Table 3, high conversion rate does not lead to high reaction yield. The poor selectivity of these catalytic systems indicates that over-oxidation of phenol exists severely. This suggests that the reported complexes catalyze not only the oxidation of benzene, but also the further oxidation of the product phenol. In fact, GC-MS results showed the formation of benzoquinone and catechol, which then could be further degraded by iron species in the catalytic process.<sup>39</sup> This may explain that all the iron complexes do not exhibit good selectivity for the production of phenol.

As mentioned earlier, in the catalysis the binding of the oxidant  $\text{H}_2\text{O}_2$  with the metal centre of the catalyst is one of the essential steps. Thus the electron density of metal centre would correlate to the catalysis. To probe the electron density, examining the

electrochemistry of the catalysts, particularly the reduction processes, is of importance. It is known that the higher the electron density, the more negative the reduction potentials of the catalysts. As shown in Table 3, the conversion rate of benzene correlates well with the reduction potentials of complexes  $\text{Fe}_1$ - $\text{Fe}_4$ . With a slight variation in ligating donor set in complex  $\text{Fe}_4$ , these complexes adopt essentially a similar geometry and coordinating environment, thus the electron density of the metal centre is the key factor determining the catalytic behaviors of these complexes. The correlation suggests that increasing the electron-donating capability of the ligands coordinating to the metal centre is beneficial to improving the catalysis. For comparison, the catalytic performance of  $\text{FeCl}_3$  was also examined as shown in Table 3. It is inferior to all the complexes in both conversion rate and yield / selectivity. Although its reduction potential in acetonitrile is more negative than that of  $\text{Fe}_4$ , its catalysis is poorer. This is probably due to the polynuclear nature and / or non-octahedral geometry,<sup>40</sup> which are different from the mononuclear complexes which are of octahedral coordination.

It is believed that iron (II) catalysts form  $\text{Fe}(\text{II})\text{-OOH}$  species and involves radical mechanism when  $\text{H}_2\text{O}_2$  is used as an oxidant.<sup>41</sup> When PhIO is used as an oxidant, high valent iron-oxo species  $\text{Fe}(\text{IV}=\text{O})$  is involved and alternative mechanism is adopted. To shed some light on possible mechanism in the oxidation of benzene catalyzed by  $\text{Fe}_1$ - $\text{Fe}_4$ , the simple radical quencher (ethanol) was used in the catalysis, Table 3. Indeed, the presence of ethanol decreases significantly the conversion rate and yield / selectivity. But further addition of ethanol by another 1 mL changed hardly the catalytic performance. This observation may suggest that another catalytic mechanism parallel to the radical one may also exists, for example, involving high valent iron-oxo species.

## 4. Conclusions

In summary, we have reported the synthesis, characterization and catalysis on the oxidation of benzene into phenol of four  $\text{Fe}(\text{III})$  complexes derived from bis(pyridin-2-ylmethyl)amine ( $\text{L}_1$ ) and its derivatives ( $\text{L}_2$  and  $\text{L}_3$ ). Structural analysis indicates that all the complexes adopt an octahedral geometry. These complexes catalyze the oxidation of benzene to phenol at moderate temperature. They catalyze also the further oxidation of phenol using  $\text{H}_2\text{O}_2$  as an oxidant which leads to the poor selectivity of the oxidation. The catalysis involves certainly radical mechanism without ruling out alternative mechanism. The catalytic activity of the four complexes correlates positively to the electron density of the metal centre. This correlation indicates that in the design of iron (III)-based catalysts, increasing the electron-donating capability of a ligand to coordinate to  $\text{Fe}(\text{III})$  is certainly beneficial. Although the conversion rate are comparable to the reported ones,<sup>23, 42, 43</sup> the selectivity is poor which is caused by over oxidation of the product. Therefore, how to avoid over oxidation becomes one of the major issues in designing  $\text{Fe}(\text{III})$ -based catalysts for the direct oxidation of benzene to phenol.

## Acknowledgments



We thank the National Natural Science Foundation of China (Grant Nos. 21171073, 21301071), the Natural Science Foundation of Zhejiang Province (LQ13B010002) and the Government of Zhejiang Province (Qianjiang professorship for XL) for supporting this work.

## Notes and references

- <sup>a</sup> Department of Chemistry, Nanchang University, Nanchang, Jiangxi 330031, China.
- <sup>b</sup> College of Biological, Chemical Sciences and Engineering, Jiaxing University, Jiaxing, Zhejiang 314001, China. Tel./Fax: +86(0)573 83643937; E-mail: xiaoming.liu@mail.zjxu.edu.cn.
- <sup>c</sup> State Key Laboratory of Coordination Chemistry, School of Chemistry and Chemical Engineering, Nanjing University, Nanjing, Jiangsu 210093, China.
- <sup>†</sup> Electronic Supplementary Information (ESI) available: For UV-vis spectra of complexes **Fe<sub>1</sub>-Fe<sub>4</sub>**, optimization of the catalytic reaction conditions and NMR copies of ligands see DOI: 10.1039/b000000x/
- P. R. O. d. Montellano, Plenum, New York, 2nd edn., 1995, p. 269.
  - B. J. Wallar and J. D. Lipscomb, *Chem. Rev.*, 1996, **96**, 2625–2658.
  - P. M. Vignais and B. Billoud, *Chem. Rev.*, 2007, **107**, 4206–4272.
  - M. Weber and M. Kleine-Boymann, in *Ullmann's Encyclopedia of Industrial Chemistry*, 2004.
  - K. Lemke, H. Ehrlich, U. Lohse, H. Berndt and K. Jähnisch, *Appl. Catal. A-Gen.*, 2003, **243**, 41–51.
  - R. Molinari and T. Poerio, *Asia-Pac. J. Chem. Eng.*, 2010, **5**, 191–206.
  - P. T. Tanev, M. Chibwe and T. J. Pinnavaia, *Nature*, 1994, **368**, 321–323.
  - L. Balducci, D. Bianchi, R. Bortolo, R. D'Aloisio, M. Ricci, R. Tassinari and R. Ungarelli, *Angew. Chem. Int. Ed.*, 2003, **42**, 4937–4940.
  - D. Bianchi, L. Balducci, R. Bortolo, R. D'Aloisio, M. Ricci, G. Spano, R. Tassinari, C. Tonini and R. Ungarelli, *Adv. Synth. Catal.*, 2007, **349**, 979–986.
  - R. J. Kalbasi, A. R. Massah, F. Zamani, A. D. Bain and B. Berno, *J. Porous Mater.*, 2011, **18**, 475–482.
  - A. N. Kharat, S. Moosavikia, B. T. Jahromi and A. Badiei, *J. Mol. Catal. A-Chem.*, 2011, **348**, 14–19.
  - X. Y. Qi, J. Y. Li, T. H. Ji, Y. J. Wang, L. L. Feng, Y. L. Zhu, X. T. Fan and C. Zhang, *Microporous Mesoporous Mater.*, 2009, **122**, 36–41.
  - H. Kanzaki, T. Kitamura, R. Hamada, S. Nishiyama and S. Tsuruya, *J. Mol. Catal. A-Chem.*, 2004, **208**, 203–211.
  - K. M. Parida and D. Rath, *Appl. Catal. A-Gen.*, 2007, **321**, 101–108.
  - A. Dubey and S. Kannan, *Catal. Commun.*, 2005, **6**, 394–398.
  - S. Q. Song, H. X. Yang, R. C. Rao, H. D. Liu and A. M. Zhang, *Appl. Catal. A-Gen.*, 2010, **375**, 265–271.
  - S. Q. Song, S. J. Jiang, R. C. Rao, H. X. Yang and A. M. Zhang, *Appl. Catal. A-Gen.*, 2011, **401**, 215–219.
  - D. Bianchi, R. Bortolo, R. Tassinari and et al, *Angew. Chem. Int. Ed.*, 2000, **39**, 4321–4323.
  - M. C. Esmelindro, E. G. Oestreich, M. Caovilla, J. A. Lessa, C. Fernandes, C. Dariva, S. M. Egues, A. J. Bortoluzzi and O. A. C. Antunes, *J. Braz. Chem. Soc.*, 2006, **17**, 1551–1557.
  - C. Detoni, N. F. Carvalho, R. M. A. Souza, D. G. Aranda and O. A. C. Antunes, *Catal. Lett.*, 2009, **129**, 79–84.
  - A. Conde, M. M. Diaz-Requejo and P. J. Perez, *Chem. Commun.*, 2011, **47**, 8154–8156.
  - C. Walling and R. A. Johnson, *J. Am. Chem. Soc.*, 1975, **97**, 363–367.
  - E. V. Kudrik and A. B. Sorokin, *Chem. Eur. J.*, 2008, **14**, 7123–7126.
  - R. R. Fernandes, M. V. Kirillova, J. A. L. da Silva, J. J. R. Frausto da Silva and A. J. L. Pombeiro, *Appl. Catal. A-Gen.*, 2009, **353**, 107–112.
  - B. Meunier, S. P. de Visser and S. Shaik, *Chem. Rev.*, 2004, **104**, 3947–3980.
  - K. H. Mitchell, C. E. Rogge, T. Gierahn and B. G. Fox, *Proc. Natl. Acad. Sci. USA*, 2003, **100**, 3784–3789.
  - L. M. Rossi, A. Neves, A. J. Bortoluzzi, R. Hörner, B. Szpoganicz, H. Terenzi, A. S. Mangrich, E. Pereira-Maia, E. E. Castellano and W. Haase, *Inorg. Chim. Acta*, 2005, **358**, 1807–1822.
  - D. Gonzalez Cabrera, B. D. Koivisto and D. A. Leigh, *Chem. Commun.*, 2007, 4218–4220.
  - S. Huang, R. J. Clark and Z. L., *Org. Lett.*, 2007, **9**, 4999–5002.
  - R. Viswanathan, M. Palaniandavar, T. Balasubramanian and P. T. Muthiah, *Journal of the Chemical Society, Dalton Trans.*, 1996, 2519–2525.
  - G. M. Sheldrick, *Acta Crystallogr., Sect. A: Found. Crystallogr.*, 2008, **64**, 112–122.
  - X. Zeng, Z. Li and X. Liu, *Electrochim. Acta*, 2010, **55**, 2179–2185.
  - X. Zeng, Z. Li, Z. Xiao, Y. Wang and X. Liu, *Electrochem. Commun.*, 2010, **12**, 342–345.
  - A. D. Becke, *Phys. Rev. A*, 1988, **38**, 3098–3100.
  - J. P. Perdew, *Phys. Rev. B*, 1986, **33**, 8822–8824.
  - J. Li, C. L. Fisher, J. L. Chen, D. Bashford and L. Noodleman, *Inorg. Chem.*, 1996, **35**, 4694–4702.
  - M. J. T. Frisch, G. W. Trucks, H. B. Schlegel, G. E. Scuseria, M. A. Robb, J. R. Cheeseman, J. A. Montgomery, Jr. T. Vreven, K. N. Kudin, J. C. Burant, J. M. Millam, S. S. Iyengar, J. Tomasi, V. Barone, B. Mennucci, M. Cossi, G. Scalmani, N. Rega, G. A. Petersson, H. Nakatsuji, M. Hada, M. Ehara, K. Toyota, R. Fukuda, J. Hasegawa, M. Ishida, T. Nakajima, Y. Honda, O. Kitao, H. Nakai, M. Klene, X. Li, J. E. Knox, H. P. Hratchian, J. B. Cross, V. Bakken, C. Adamo, J. Jaramillo, R. Gomperts, R. E. Stratmann, O. Yazyev, A. J. Austin, R. Cammi, C. Pomelli, J. W. Ochterski, P. Y. Ayala, K. Morokuma, G. A. Voth, P. Salvador, J. J. Dannenberg, V. G. Zakrzewski, S. Dapprich, A. D. Daniels, M. C. Strain, O. Farkas, D. K. Malick, A. D. Rabuck, K. Raghavachari, J. B. Foresman, J. V. Ortiz, Q. Cui, A. G. Baboul, S. Clifford, J. Cioslowski, B. B. Stefanov, G. Liu, A. Liashenko, P. Piskorz, I. Komaromi, R. L. Martin, D. J. Fox, T. Keith, M. A. Al-Laham, C. Y. Peng, A. Nanayakkara, M. Challacombe, P. M. W. Gill, B. Johnson, W. Chen, M. W. Wong, C. Gonzalez and J. A. Pople, *Gaussian 03*, 2003, Revision E.01.
  - E. A. Mikhalyova, O. V. Makhlynets, T. D. Palluccio, A. S. Filatov and E. V. Rybak-Akimova, *Chem. Commun.*, 2012, **48**, 687–689.
  - J. Liu, Z. H. Wei, W. Zhong, W. M. Liu, X. Liu and X. M. Liu, *Chin. J. Inorg. Chem.*, 2013, **29**, 2205–2214.
  - F. A. Cotton and G. Wilkinson, in *Advanced Inorganic Chemistry*, Wiley-interscience, New York, 1988, p. 713.
  - N. Segaud, J. N. Rebilly, K. Senechal-David, R. Guillot, L. Billon, J. P. Baltaze, J. Farjon, O. Reinaud and F. Banse, *Inorg. Chem.*, 2013, **52**, 691–700.
  - D. Bianchi, M. Bertoli, R. Tassinari, M. Ricci and R. Vignola, *J. Mol. Catal. A-Chem.*, 2003, **204**, 419–424.
  - L. Chen, Y. Xiang and T. Feng, *Appl. Organomet. Chem.*, 2012, **26**, 108–113.

**Table 1** Crystallographic details for complexes **Fe<sub>1</sub>-Fe<sub>4</sub>**.

	<b>Fe<sub>1</sub></b>	<b>Fe<sub>2</sub></b>	<b>Fe<sub>3</sub></b>	<b>Fe<sub>4</sub></b>
Empirical formula	C <sub>12</sub> H <sub>13</sub> Cl <sub>3</sub> FeN <sub>3</sub>	C <sub>15</sub> H <sub>15</sub> Cl <sub>3</sub> FeN <sub>3</sub>	C <sub>22</sub> H <sub>22</sub> Cl <sub>3</sub> FeN <sub>6</sub> ·0.5CH <sub>2</sub> Cl <sub>2</sub>	C <sub>22</sub> H <sub>22</sub> Cl <sub>3</sub> F <sub>6</sub> FeN <sub>6</sub> P
<i>F<sub>w</sub></i>	361.45	399.50	575.12	642.18
Crystal system	Orthorhombic	Monoclinic	Orthorhombic	Monoclinic
space group	<i>Pna2(1)</i>	<i>P2(1)/c</i>	<i>Fdd2</i>	<i>P2(1)/n</i>

a/Å	15.6262 (18)	13.725 (2)	30.029 (4)	8.9480(8)
b/Å	8.4836 (10)	14.961 (2)	33.845 (5)	8.8509(8)
c/Å	22.772 (3)	8.2443 (12)	9.7572 (14)	32.824(3)
$\alpha$ (°)	90	90	90	90
$\beta$ (°)	90	92.129(2)	90	96.0490(10)
$\gamma$ (°)	90	90	90	90
$V$ , Å <sup>3</sup>	3018.8 (6)	1691.7(4)	9917 (2)	2585.1 (4)
$Z$	8	4	16	4
$D_{\text{calc}}$ , Mg/m <sup>3</sup>	1.591	1.569	1.541	1.650
$F(000)$	1464	812	4704	1300
Reflections collected	17373	15797	19600	23978
Reflections independent( $R_{\text{int}}$ )	5879, 0.0179	4245, 0.0166	4132, 0.0337	6400, 0.0437
Goodness-of-fit on $F^2$	1.048	1.039	1.089	1.023
$R_1$ , $wR_2$ [ $I > 2\sigma(I)$ ]	0.0212, 0.0553	0.0233, 0.0624	0.0275, 0.0712	0.0544, 0.1251
$R_1$ , $wR_2$ (all data)	0.0234, 0.0563	0.0271, 0.0650	0.0285, 0.0776	0.0940, 0.1437

**Table 2** Contrast of bond lengths (Å) and angles (°) for complexes **Fe<sub>1</sub>-Fe<sub>4</sub>**.

lengths (Å)	<b>Fe<sub>1</sub></b>	<b>Fe<sub>2</sub></b>	<b>Fe<sub>3</sub></b>	<b>Fe<sub>4</sub></b>
Fe(1)-N(1)	2.210(2)	2.304(1)	2.257(2)	2.261(3)
Fe(1)-N(2)	2.197(2)	2.186(1)	2.191(3)	2.158(3)
Fe(1)-N(3)	2.187 (2)	2.202(1)	2.167(2)	2.121(3)
Fe(1)-N(4)				2.143(3)
Fe(1)-Cl(1)	2.279(7)	2.261(4)	2.295(8)	2.244(1)
Fe(1)-Cl(2)	2.289(7)	2.307 (5)	2.299 (8)	2.262(1)
Fe(1)-Cl(3)	2.318(7)	2.314 (5)	2.286 (9)	
angles (°)	<b>Fe<sub>1</sub></b>	<b>Fe<sub>2</sub></b>	<b>Fe<sub>3</sub></b>	<b>Fe<sub>4</sub></b>
N(3)-Fe(1)-N(2)	78.77(7)	87.64(4)	81.02(9)	151.63(1)
N(3)-Fe(1)-N(1)	76.39(8)	73.27(4)	78.44(8)	76.39(1)
N(2)-Fe(1)-N(1)	76.31(7)	76.03(4)	75.27(9)	75.29(1)
N(3)-Fe(1)-Cl(2)	92.30(6)	90.28(3)	166.08(7)	92.43(8)
N(2)-Fe(1)-Cl(2)	164.46(5)	166.68(3)	88.04(6)	90.77(8)
N(1)-Fe(1)-Cl(2)	89.30(6)	90.78(3)	90.51(6)	93.12(8)
N(3)-Fe(1)-Cl(1)	93.53(6)	92.57(3)	92.99(7)	103.36(8)
N(2)-Fe(1)-Cl(1)	94.35(5)	94.09(3)	94.72(6)	103.76(8)
N(1)-Fe(1)-Cl(1)	167.32(6)	162.83(3)	167.63(7)	166.43(8)
N(3)-Fe(1)-Cl(3)	162.54(6)	166.18(3)	90.83 (7)	
N(2)-Fe(1)-Cl(3)	87.16(5)	84.08(3)	166.87(6)	
N(1)-Fe(1)-Cl(3)	90.36(6)	93.95(3)	93.09 (7)	
Cl(2)-Fe(1)-Cl(3)	98.95(3)	95.23(2)	98.28(3)	
Cl(1)-Fe(1)-Cl(3)	97.82(3)	99.02(2)	95.98(4)	
Cl(2)-Fe(1)-Cl(1)	98.91(3)	99.14(2)	96.48(3)	100.44(4)
N(4)-Fe(1)-Cl(1)				89.76(7)
N(4)-Fe(1)-Cl(2)				169.26(8)
N(4)-Fe(1)-N(1)				76.67(1)
N(4)-Fe(1)-N(2)				83.49(1)
N(3)-Fe(1)-N(4)				88.42(1)

**Table 3** Oxidation of benzene with H<sub>2</sub>O<sub>2</sub> using various catalysts under the optimized reaction conditions.

	<sup>c</sup> Ep	Conversion	Selectivity	Yield	TON	TOF/ h <sup>-1</sup>
<b>Fe<sub>1</sub></b>	-0.433	42.0%	26.8%	11.2%	56	28
<b>Fe<sub>2</sub></b>	-0.363	37.7%	52.9%	19.9%	100	50
<b>Fe<sub>3</sub></b>	-0.330	35.2%	34.7%	12.2%	61	30
<b>Fe<sub>4</sub></b>	-0.210	31.5%	41.2%	13.0%	65	32
FeCl <sub>3</sub>	-0.235	26.7%	34.4%	9.2%	46	23
<sup>a</sup> <b>Fe<sub>2</sub></b>	/	17.1%	35.5%	6.0%	30	15
<sup>b</sup> <b>Fe<sub>2</sub></b>	/	16.9%	24.2%	4.1%	20	10

<sup>a</sup> 1 mL of ethanol was added while the total volume of the reaction mixture was kept unchanged. <sup>b</sup> 2 mL of ethanol was added.